



EERA DeepWind' 2014, 11th Deep Sea Offshore Wind R&D Conference

Fatigue Reliability-Based Inspection and Maintenance Planning of Gearbox Components in Wind Turbine Drivetrains

Amir Rasekhi Nejad*, Zhen Gao, Torgeir Moan

Norwegian Research Centre for Offshore Wind Technology (Nowitech) and Centre for Ships and Ocean Structures (CeSOS), Norwegian University of Science and Technology (NTNU), NO-7491, Trondheim, Norway

Abstract

This paper introduces a reliability-based maintenance plan for wind turbine gearbox components. The gears and bearings are graded based on their fatigue damage and a maintenance map is developed to focus on those components with higher probability of fatigue failure and lower level of reliability. The main aim of this paper is to propose a method for developing the "vulnerability map" which can be used by maintenance teams to identify the components with lower reliabilities. The fatigue damage for gears and bearings are calculated at rated wind speed by the SN curve approach. The load duration distribution (LDD) method is used to obtain the stress range cycles for gears and load range cycles for bearings from the load and load effect time series obtained from a global response analysis. During routine inspection and maintenance, the vulnerability map can be used to find the faulty component by inspecting those with highest probability of failure rather than examining all gears and bearings. Such maps can be used for fault detection during routine maintenance and can reduce the down time and efforts of maintenance team to identify the source of problem. The proposed procedure is exemplified by a 750 kW gearbox and a vulnerability map is developed for this case study gearbox.

© 2014 Elsevier Ltd. This is an open access article under the CC BY-NC-ND license (<http://creativecommons.org/licenses/by-nc-nd/3.0/>).

Selection and peer-review under responsibility of SINTEF Energi AS

Keywords: wind turbine gears; fault detection; drivetrain; maintenance

1. Introduction

Maintenance, in general terms, is classified into corrective and precautionary - or preventive - actions [1]. The corrective action is taken when the failure of components is occurred and the system is partly broken down. While the preventive maintenance action is on routine schedule to repair or replace components before they fail [2]. Apart from unscheduled repairs which are identified by condition monitoring systems, the preventive maintenance of wind turbine gearboxes is often carried every 6 months for each wind turbine, normally within a day, and a major check-up is performed every 3 years. The wind turbine gearbox routine inspections include oil sampling for particle counting, oil filter checking, observing the possible oil leakage from housing or pipes and identifying any unusual noise from

* Corresponding author. Tel.: +47-735-91546 ; fax: +47-735-95528.
E-mail address: Amir.Nejad@ntnu.no.

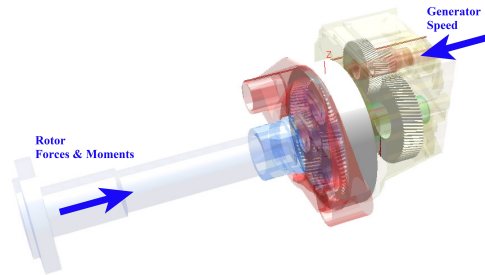


Fig. 1. MBS model of 750 kW gearbox.

the gearbox [3]. The oil sampling is often offline, even in offshore wind turbines equipped with condition monitoring systems. If the result indicates high debris in the oil, unusual noise or leakage, further internal visual inspection by other means such as endoscope or fiberscope with camera is then performed [3].

In the endoscope or fiberscope inspection, the maintenance inspector should examine all gears and bearings, one by one in order to find the source of noise or debris in the oil. Any knowledge of impending failure can reduce cost dramatically and can help the maintenance team to plan [4]. The components with higher fatigue damage are those with higher probability of failure. Therefore, it is reasonable that the inspection follows a plan which highlights those with the lowest reliability level. In this paper, the procedure to create such plans is demonstrated and exemplified for a 750 kW gearbox. Such vulnerability map should be produced by the gearbox designer in the design stage and made available to the maintenance team. Moreover, it can be used in conjunction with condition monitoring data to find the potential failures, provided that the turbine is fitted with condition monitoring systems.

2. 750 kW Gearbox Model

In this paper, the proposed method is exemplified by a 750 kW gearbox obtained from the Gearbox Reliability Collaborative (GRC) project at the National Renewable Energy Laboratory (NREL). The wind turbine and gearbox data are provided in Appendix A. The loads on gears and bearings are obtained from the decoupled analysis. More information about this method can be found in Nejad et al. [5,6]. The global loads on the drivetrain are measured using a NREL dynamometer test bench. Next, these loads are used as inputs to a multibody system (MBS) drivetrain model in SIMPACK [7]. See Fig. 1 for an illustration of the drivetrain MBS model. The main shaft loads, or the forces and moments, are applied at the end of the main shaft where the rotor hub is connected.

The 750 kW GRC gearbox consists of one planetary stage and two parallel helical stages. Fig. 2 presents the gear arrangement and bearings. Sixty-second measurements of forces and moments in a steady-state, non-transient condition under 100% torque representing the rated wind speed condition, are collected from the dynamometer test bench. The input measurement is then applied on the MBS model and a simulation with time steps of 0.005 sec. (seconds) is performed. The first 10 sec. of data are removed to avoid numerical convergence uncertainties. In the earlier work by Nejad et al. [6], it is shown that the rated wind speed has the biggest contribution in fatigue damage of the gearbox. Therefore, the bearing and gear fatigue damage at rated wind speed is used for damage calculations.

The MBS model used in this paper has been used in many earlier studies and been verified by experimental data. [8–10]. More details about the GRC gearbox model can be found in NREL's reports [11,12].

3. Theory and Methodology

3.1. Failure Modes

The failure modes of wind turbine gearbox assembly identified through failure modes and effects analysis (FMEA) in ReliaWind project [13,14] includes: planetary gear failure, high speed shaft bearing failure, planetary bearing

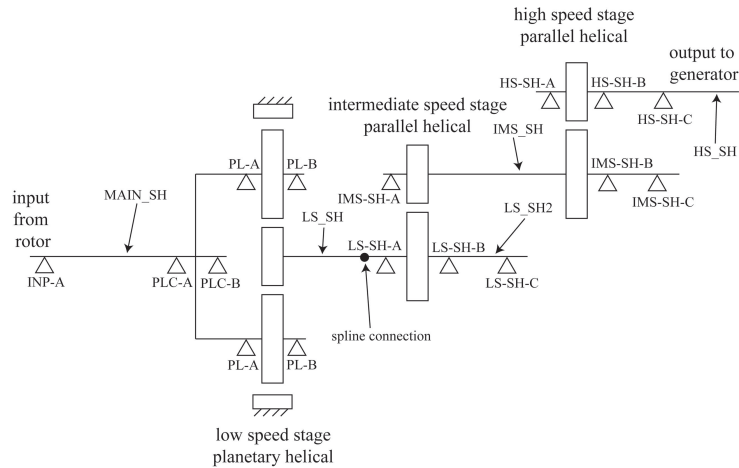


Fig. 2. 750 kW gearbox topology.

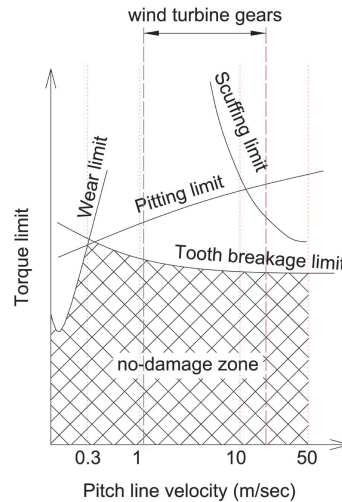


Fig. 3. Failure modes of wind turbine gears (adapted after Niemann [19]).

failure and intermediate shaft bearing failure. The gear failure is in two general groups of lubrication-related or strength-related classes [15]. The gear most common types of failure are cited by American gear manufacturing association (AGMA) [16] into seven broad headings of: wear, scuffing, plastic deformation, contact fatigue, cracking, fracture and bending fatigue. Some gear failure modes, particularly in lubrication-related category, are long processes e.g. wear, scuffing and contact fatigue. Tooth fracture may occur under extreme loads or as highlighted by ISO 10825 [17] the overloading can create cracks in the root which are later progressing as root bending fatigue cracks with slow propagation. The consequences of failure modes are also not the same. For instance, the consequences of gear tooth fracture due to bending fatigue or overloading are severe. The broken tooth particle damages other teeth and can lead to the gearbox progressive collapse, while pitting damage may only increase the gearbox vibration and noise. According to ISO 6336-2 [18], the tolerable extent of pitting damage depends on the gear application.

Moreover, as it is shown in Fig. 3, the tooth breakage may occur earlier than pitting as torque increase. Therefore, the gear tooth root bending fatigue damage has been used as the criteria in this paper.

The ball or roller bearings, known more generally as anti-friction bearings, are the most common bearings used in wind turbine gearboxes and consist of rollers, balls, races and supporting cases. Rolling bearing life is limited by the fatigue life of the internal components and is modified by the lubricant used. The fatigue life of bearings is established based on the Lundberg-Palmgren hypothesis [10] which is described in the following sections.

3.2. Gear Fatigue Damage Calculation

The gear tooth root bending fatigue damage (D) can be estimated based on the Palmgren-Miner hypothesis of linear damage and SN curve data by [6]:

$$D = \frac{N_T}{K_c} \int_0^{+\infty} s^m f(s) ds = \frac{N_T}{K_c} A^m \Gamma\left(1 + \frac{m}{B}\right) \quad (1)$$

where $\Gamma()$ is a gamma function and A and B are Weibull shape and scale parameters of the form:

$$F_S(s) = 1 - \exp\left(-\left(\frac{s}{A}\right)^B\right) \quad (2)$$

in which $F_S(s)$ is the Weibull cumulative distribution function of the short-term stress range. N_T is the total number of cycle in the simulation period. K_c and m are material parameters from design SN curves [20]. The stress range number of cycles is calculated by load duration distribution (LDD) method. More details about this method can be found in Nejad et al. [6].

3.3. Bearing Fatigue Damage Calculation

The bearing design is generally based on the desired life and damage formulation established by Lundberg-Palmgren [21]:

$$PL^{\frac{1}{a}} = const. \quad (3)$$

where L is bearing life, P the applied radial load on the bearing over a given period, $a = 3$ for ball bearing and $a = \frac{10}{3}$ for roller bearings such as PL-A and PL-B, see Fig. 2. Manufacturer bearing catalogues contain the basic life and load ratings established from laboratory tests. The relationship between a manufacturers data and the desired design parameters is expressed by:

$$LP^a = L_{10}C^a = const. \quad (4)$$

where L_{10} is the characteristic basic rating life defined as the number of cycles that 90% of an identical group of bearings achieves, under a certain test conditions, before the fatigue damage appears. C is the basic load rating and constant for a given bearing. P is the dynamic equivalent radial load calculated from $P = XF_r + YF_a$, and F_a and F_r are the axial and radial loads on the bearing respectively, X and Y are constant factors taken from ISO 281 [22]. In the case of planet bearings, PL-A and PL-B, $X = 1.0$ and $Y = 0.0$.

Equation (4) is one form of the single SN curve formulation for high-cycle fatigue. The fatigue damage is often calculated using Palmgren-Miners hypothesis of linear cumulative damage, given by:

$$D = \sum_i \frac{l_i}{L_i} \quad (5)$$

where D is the accumulated fatigue damage for a load time history with duration T , l_i is the number of load cycles in the time history associated with load range P_i , and L_i is taken from equation (4) given as $L_i = \frac{L_{10}C^a}{P_i^a}$, which represents

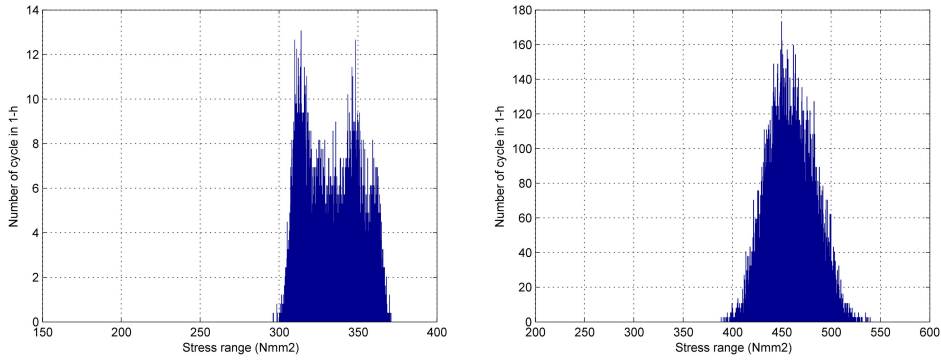


Fig. 4. Stress range and number of stress cycles, planet gear (left); 3rd stage gear (right).

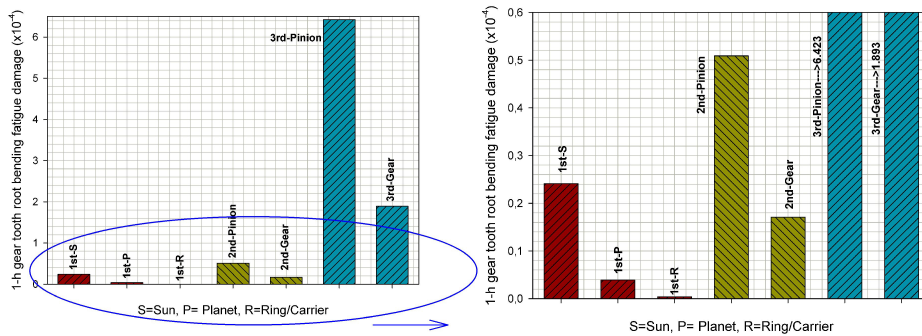


Fig. 5. 1-h gear tooth root bending fatigue damage.

the number of load cycles to failure at a load range of P_i . The short-term fatigue damage, D can be expressed by e.g. [23,24]:

$$D = \sum_i \frac{l_i}{L_i} = \frac{v_{p0}T}{L_{10}C^a} \int_0^{+\infty} p^a f_P(p) dp \tag{6}$$

where $f_P(p)$ is the short-term probability density function of load range P , T is the short-term period in hours and v_{p0} is the number of load cycles in one hour. If $f_P(p)$ is fitted by a 2-parameter Weibull distribution, the fatigue damage can be obtained analytically by:

$$D = \frac{v_{p0}T}{L_{10}C^a} A^a \Gamma\left(1 + \frac{a}{B}\right) \tag{7}$$

where $\Gamma()$ is a gamma function and A and B are Weibull shape and scale parameters. It should be noted that the method described herein is the most common approach for bearing life calculation. More refined methods considering internal components can be found in Jiang et al. [25].

4. Results

The fatigue damages of gears and bearings in the 750 kW case study gearbox are calculated. The LDD method is used for bearing load and gear stress cycle counting. Fig. 4 presents the number of cycles in 1-h as a function of stress range for planet gear and 3rd stage gearwheel. The 1-h fatigue damage of the gears at rated wind speed is shown in Table 1 and illustrated in Fig. 5.

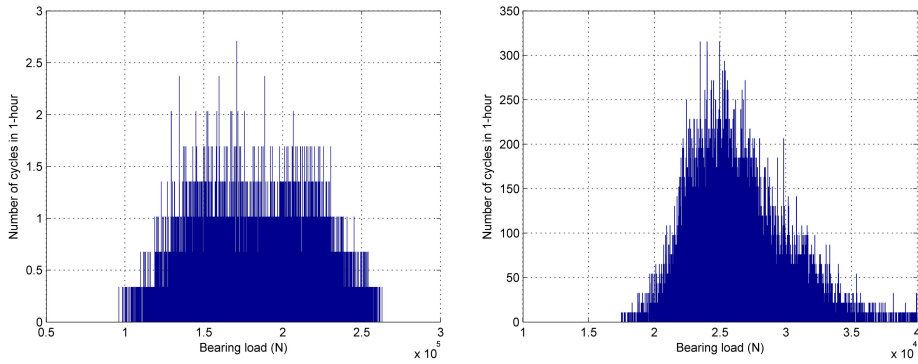


Fig. 6. Load range and number of load cycles, planet bearing (PL-B) (left); high speed shaft bearing (HS-SH-C) (right).

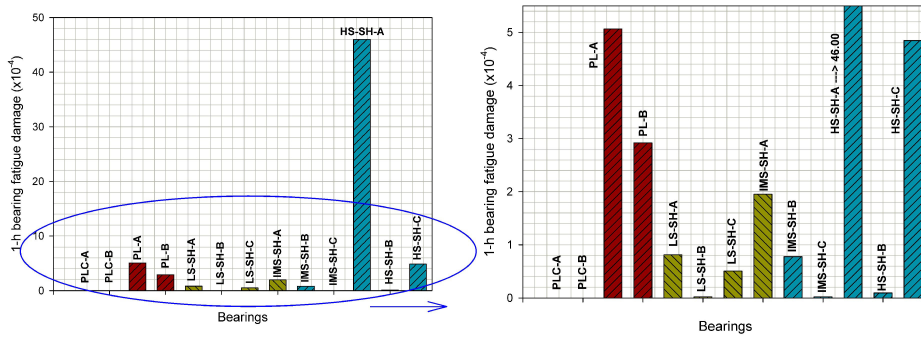


Fig. 7. 1-h bearing fatigue damage.

Table 1. 1-h gear tooth root bending fatigue damage.

Stage	Gear	$D (\times 10^{-4})$
1 st stage	Sun gear	0.241
	Planet gear	0.039
	Ring gear	0.004
2 nd stage	Pinion	0.509
	Gear	0.171
3 rd stage	Pinion	6.423
	Gear	1.893

The gears in the 3rd stage are found those with the highest fatigue damage. The reason primarily lies on the high number of cycles in this stage. Moreover, the variation of the damage in the 1st stage is due to the geometrical restriction in planetary systems [6].

The bearing fatigue damage is presented in Table 2 and Fig. 7. The number of load cycle versus load range for planet bearing and high speed shaft bearing is also shown in Fig. 6.

The highest fatigue damage is observed at the 3rd stage bearing, HS-SH-A and the lowest at planet carrier bearings, PLC-A and PLC-B. In Table 3, the bearings and gears are sorted based on their fatigue damage from the highest to the lowest. From this information, the "vulnerability map" can now be constructed, see Fig. 8. In this map, Fig. 8, bearings and gears are highlighted in colour representing their fatigue damage level.

Table 2. 1-h bearing fatigue damage.

Stage	Bearing	$D (\times 10^{-4})$
1 st stage	PLC-A	0.000
	PLC-B	0.000
	PL-A	5.064
	PL-B	2.921
2 nd stage	LS-SH-A	0.812
	LS-SH-B	0.020
	LS-SH-C	0.507
	IMS-SH-A	1.954
3 rd stage	IMS-SH-B	0.777
	IMS-SH-C	0.021
	HS-SH-A	46.00
	HS-SH-B	0.096
	HS-SH-C	4.846

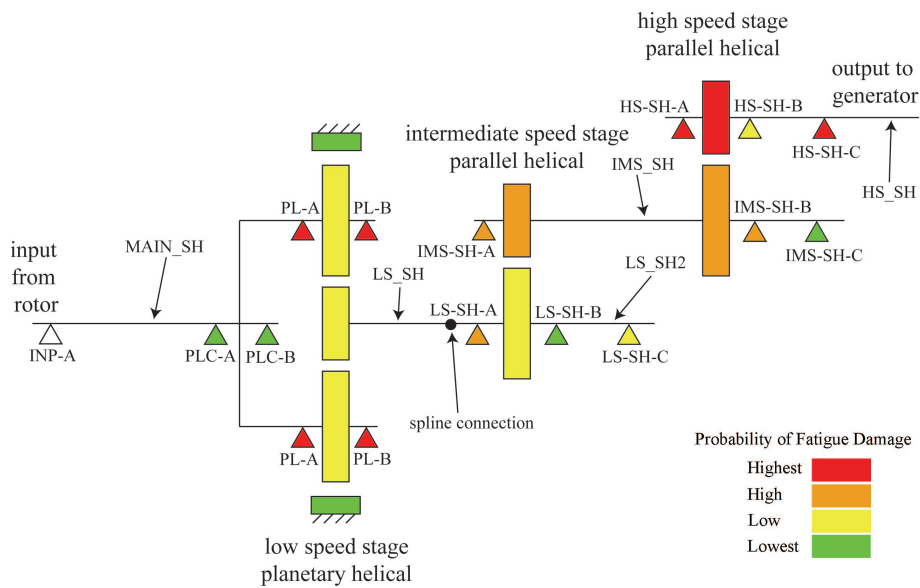


Fig. 8. "vulnerability map" of 750 kW case study gearbox based on component fatigue damage ranking.

5. Concluding Remarks

In this paper an inspection and maintenance planning map based on the fatigue damage of gears and bearings is presented. The procedure for calculating the short-term fatigue damage for gears and bearings is described and exemplified for the NREL GRC 750 kW gearbox. The gearbox components are then sorted based on their fatigue damage. A "vulnerability map" is constructed indicating the components with highest to lowest fatigue damage. This maintenance map can be used for maintenance planning and inspection of components during routine preventive maintenance inspections. This approach can give the advantage of detecting the source of fault in shorter time. By using this plan, the maintenance inspector looks for defects from those with higher probability of failure, rather than examining all gears and bearings.

It is emphasized that the vulnerability map demonstrated herein is wind turbine specific and should not be generalized for other gearboxes. Moreover, ideally one should use the long-term fatigue damage estimation – for instance by the method described by Nejad et al. [6] – for gear and bearing design and maintenance planning. It is therefore

Table 3. Gears and bearings sorted based on 1-h fatigue damage at rated wind speed.

Rank	Gear or Bearing	Name	$D (\times 10^{-4})$
1	Bearing	HS-SH-A	46.00
2	Gear	3rd Pinion	6.423
3	Bearing	PL-A	5.064
4	Bearing	HS-SH-C	4.846
5	Bearing	PL-B	2.921
6	Bearing	IMS-SH-A	1.954
7	Gear	3rd Gear	1.893
8	Bearing	LS-SH-A	0.812
9	Bearing	IMS-SH-B	0.777
10	Gear	2nd Pinion	0.509
11	Bearing	LS-SH-C	0.507
12	Gear	1st Sun Gear	0.241
13	Gear	2nd Gear	0.171
14	Bearing	HS-SH-B	0.096
15	Gear	1st Planet Gear	0.039
16	Bearing	IMS-SH-C	0.021
17	Bearing	LS-SH-B	0.020
18	Gear	1st Ring Gear	0.004
19	Bearing	PLC-A	0.000
20	Bearing	PLC-B	0.000

proposed to devote future work to develop vulnerability maps based on long-term fatigue and for different gearboxes in different sites and sizes.

Acknowledgements

The authors wish to acknowledge financial support from the Research Council of Norway through the Norwegian Research Centre for Offshore Wind Technology (Nowitech) and the Centre for Ships and Ocean Structures (CeSOS). The gearbox and wind turbine model was obtained courtesy of the Gearbox Reliability Collaborative (GRC) project at the National Renewable Energy Laboratory, Colorado, USA. The GRC initiative is funded by the Wind and Water Power Program of the United States Department of Energy. The first author would also like to thank Dr. Y. Xing, a former colleague at CeSOS, for providing initial MBS models and Dr. Y. Guo from GRC/NREL for valuable discussions.

Appendix A. 750 kW case study gearbox technical data

The 750 kW wind turbine and gearbox technical descriptions are listed in Tables A1,A2.

Table A1. NREL 750 kW wind turbine description.

Description	Value
Type	3 blades, upwind
Power rating (kW)	750
Rotor dia. (m)	48.2
Rated rotor speed (rpm)	22/15
Power regulation	Stall
Nominal hub height (m)	55
Cut-in wind speed (m/s)	3
Rated wind speed (m/s)	16
Cut-out wind speed (m/s)	25
Design wind class	IEC Class II
Design life (year)	20

Table A2. NREL 750 kW gearbox description.

Description	Value
Type	1Planetary+2Helical
Gearbox ratio	1:81.482
1 st stage ratio	1:5.714
2 nd stage ratio	1:3.565
3 rd stage ratio	1:4.000

References

- [1] Pintelon L, Parodi-Herz A. Maintenance: an evolutionary perspective. In: Kobbacy KAH, Murthy DNP, editors. Complex system maintenance handbook. Berlin: Springer; 2008.
- [2] Marquez FPG, Tobias AM, Perez JMP, Papaalias M. Condition monitoring of wind turbines: techniques and methods. *Renewable Energy* 2012;46:169-178.
- [3] Hockley CJ. Wind turbine maintenance and typical research questions. *Procedia CIRP* 2013;11:284-286.
- [4] Butterfield S, Sheng S, Oyague F. Wind energy's new role in supplying the world's energy: what role will structural health monitoring play? USA: National Renewable Energy Laboratory; NREL/CP-500-46180:2009, 2009.
- [5] Nejad AR, Gao Z, Moan T. Long-term analysis of gear loads in fixed offshore wind turbines considering ultimate operational loadings. *Energy Procedia* 2013;35:187-197.
- [6] Nejad AR, Gao Z, Moan T. On long-term fatigue damage and reliability analysis of gears under wind loads in offshore wind turbine drivetrains. *International Journal of Fatigue*, 2014;61:116-128.
- [7] Multibody System software, SIMPACK, www.simpack.de.
- [8] Xing Y, Moan T. Multi-body modelling and analysis of a planet carrier in a wind turbine gearbox. *Wind Energy* 2012 (DOI: 10.1002/we.1540).
- [9] Dong W, Xing Y, Moan T, Gao Z. Time domain-based gear contact fatigue analysis of a wind turbine drivetrain under dynamic conditions. *International Journal of Fatigue* 2013;48:133-146.
- [10] Nejad AR, Xing Y, Guo Y, Keller J, Gao Z, Moan T. Effect of floating sun gear in wind turbine planetary gearbox with geometrical imperfections. *Wind Energy* 2013, submitted for publication.
- [11] Oyague F, Butterfield CP, Sheng S. Gearbox Reliability Collaborative Analysis Round Robin, Technical Report. USA: National Renewable Energy Laboratory; NREL/CP-500-45325, 2009.
- [12] Link H, LaCava W, Van Dam J, McNiff B, Sheng S, Wallen R, McDade M, Lambert S, Butterfield S, Oyague F. Gearbox reliability collaborative project report: findings from phase 1 and phase 2. USA: National Renewable Energy Laboratory; NREL/CP-5000-51885, 2011.
- [13] ReliaWind. Whole system reliability model. Report no. D.2.0.4.a. 2011. Available online from: http://www.reliawind.eu/files/file-inline/110318_ReliaWind_DeliverableD.2.0.4aWhole_SystemReliabilityModel_Summary.pdf (accessed 15 Nov. 2013).
- [14] Tavner P. Offshore wind turbine reliability, availability and maintenance. 1st ed. UK: IET; 2012.
- [15] Ku PM. Gear failure modes Importance of lubrication and mechanics. *Tribology Transactions* 1976;19(3):239-249.
- [16] American Gear Manufacturers Association, AGMA 1010-E95: Appearance of gear teeth Terminology of wear and failure, USA, 1995.
- [17] International Organization for Standardization, ISO 10825: Gears Wear and damage to gear teeth terminology, Switzerland, 1995.
- [18] International Organization for Standardization, ISO 6336-2: Calculation of load capacity of spur and helical gears - Part 2: Calculation of surface durability (pitting), Switzerland, 2006.

- [19] Niemann G, Winter H. Maschinenelemente Band II: Getriebe allgemein, Zahnradgetriebe ,Grundlagen, Stirnradgetriebe. Berlin: Springer-Verlag, 1983 (in German).
- [20] International Organization for Standardization, ISO 6336-5: Calculation of load capacity of spur and helical gears - Part 5: Strength and quality of material, Switzerland, 2003.
- [21] Lundberg G, Palmgren A. Dynamic capacity of rolling bearings. Acta Polytechnica Mechanical Engineering Series 1952;2:5-32.
- [22] International Organization for Standardization, ISO 281, Rolling bearings - Dynamic load ratings and rating life, Switzerland, 2007.
- [23] Naess A, Moan T. Stochastic dynamics of marine structures. USA: Cambridge University Press, 2012.
- [24] Almar-Naess A. Fatigue handbook offshore steel structures. Norway: Tapir, 1985.
- [25] Jiang Z, Xing Y, Guo Y, Moan T, Gao Z. Long-term contact fatigue analysis of a planetary bearing in a land-based wind turbine drivetrain. Wind Energy 2014. doi: 10.1002/we.1713.